

*Short Note*On the Use of High-Resolution Topographic Data as a Proxy  
for Seismic Site Conditions ( $V_{S30}$ )

by Trevor I. Allen\* and David J. Wald

**Abstract** An alternative method has recently been proposed for evaluating global seismic site conditions, or the average shear velocity to 30 m depth ( $V_{S30}$ ), from the Shuttle Radar Topography Mission (SRTM) 30 arcsec digital elevation models (DEMs). The basic premise of the method is that the topographic slope can be used as a reliable proxy for  $V_{S30}$  in the absence of geologically and geotechnically based site-condition maps through correlations between  $V_{S30}$  measurements and topographic gradient. Here we evaluate the use of higher-resolution (3 and 9 arcsec) DEMs to examine whether we are able to resolve  $V_{S30}$  in more detail than can be achieved using the lower-resolution SRTM data. High-quality DEMs at resolutions greater than 30 arcsec are not uniformly available at the global scale. However, in many regions where such data exist, they may be employed to resolve finer-scale variations in topographic gradient, and consequently,  $V_{S30}$ . We use the U.S. Geological Survey Earth Resources Observation and Science (EROS) Data Center's National Elevation Dataset (NED) to investigate the use of high-resolution DEMs for estimating  $V_{S30}$  in several regions across the United States, including the San Francisco Bay area in California, Los Angeles, California, and St. Louis, Missouri. We compare these results with an example from Taipei, Taiwan, that uses 9 arcsec SRTM data, which are globally available.

The use of higher-resolution NED data recovers finer-scale variations in topographic gradient, which better correlate to geological and geomorphic features, in particular, at the transition between hills and basins, warranting their use over 30 arcsec SRTM data where available. However, statistical analyses indicate little to no improvement over lower-resolution topography when compared to  $V_{S30}$  measurements, suggesting that some topographic smoothing may provide more stable  $V_{S30}$  estimates. Furthermore, we find that elevation variability in canopy-based SRTM measurements at resolutions greater than 30 arcsec are too large to resolve reliable slopes, particularly in low-gradient sedimentary basins.

## Introduction

For real-time earthquake alert systems, such as the Prompt Assessment of Global Earthquakes for Response (PAGER; Earle *et al.*, 2008; Wald *et al.*, 2008), we seek to rapidly evaluate potential ground shaking in the source region and subsequently provide an estimate of the population exposure to potentially fatal levels of shaking in any region of the world. Consequently, knowledge of local seismic site conditions is an important factor in estimating ground-motion amplification potential. Wald and Allen (2007) pre-

sented a method for mapping uniform global seismic site conditions, or the average shear velocity to 30 m depth ( $V_{S30}$ ), from the Shuttle Radar Topography Mission (SRTM) 30 arcsec (approximately 1 km resolution at the equator) digital elevation model (Farr and Kobrick, 2000). This method correlates  $V_{S30}$  measurements with the topographic gradient on which they were measured to provide two sets of coefficients that can be used as predictors of  $V_{S30}$ : one for active tectonic regions where the topographic relief is youthful and dynamic and another for stable continental regions where the topography is generally more subdued. The basic premise of Wald and Allen's (2007) technique is that the topo-

\*Now at Risk and Impact Analysis Group, Geoscience, Australia GPO Box 378, Canberra ACT 2601.

graphic slope can be used as a reliable predictor of  $V_{S30}$  in the absence of geologically and geotechnically based site-condition maps. Other geoscience disciplines have used similar topography-based techniques to generate surrogate datasets, such as methods to delineate hydrologic units in depositional terrains (e.g., Gallant and Dowling, 2003).

Estimates of  $V_{S30}$  from the topographic gradient compare favorably with site-condition maps based on geology and other geomorphic and geotechnical indicators (Allen and Wald, 2007; Wald and Allen, 2007; Michelini *et al.*, 2008). To date, this method and variations of it have been adopted in several regional earthquake hazard assessments and for near real-time estimates of ground shaking (e.g., ShakeMap, Wald *et al.*, 1999), where little is known about the surficial geology and its potential effects on ground-motion amplification (e.g., Bungum *et al.*, 2007; Harmandar *et al.*, 2007; Ionescu *et al.*, 2007). In addition, new site-condition maps developed for California now employ a hybrid approach to site-condition mapping by combining geological and geotechnical information with topographic gradient as predictors of  $V_{S30}$  (Wills and Gutierrez, 2008). The U.S. Geological Survey (USGS) Global  $V_{S30}$  Server (<http://earthquake.usgs.gov/vs30/>) based on Wald and Allen's (2007) method is also a well-used service and can deliver a  $V_{S30}$  grid of any user-specified region. However, this service is currently limited by the resolution of the input digital elevation model (DEM).

Herein, we examine whether the use of high-resolution DEMs can be used to recover improved estimates of  $V_{S30}$  beyond that which can be delivered using the original correlations of Wald and Allen (2007). We also examine the differences between the SRTM data and the EROS Data Center's National Elevation Dataset (NED) for this application.

### National and Global Elevation Datasets

The National Map Seamless Server provided by the USGS EROS Data Center (<http://seamless.usgs.gov/>) allows the download of high-resolution NED digital elevation models for the United States, in addition to the global SRTM dataset (USGS, 2008). NED is designed to provide national elevation data in a seamless form with a consistent datum, elevation unit, and projection, and it uses various data corrections that minimize artifacts (Gesch *et al.*, 2002). Elevation values for NED are derived from topographic maps and aerial photographs compiled between 1925 and 1999. NED represents the best available DEM for the United States. However, maps used in NED were drawn by a number of photogrammetrists using aerial photography in a variety of scales over several decades. If vegetation obscured their view of the ground, these highly skilled experts mapped the ground surface as well as they could (J. Godt, written comm., 2008). Because the surface elevations can be ambiguous from aerial photography, minor topographic undulations were often smoothed. The digital NED has a resolution of 1 arcsec (approximately 30 m) for the conterminous United

States, Hawaii, Puerto Rico, and the island territories, and 2 arcsec for Alaska (USGS, 2008).

The SRTM data were gathered in February 2000 by the Space Shuttle Endeavor using an Interferometric Synthetic Aperture Radar (InSAR) instrument (Farr and Kobrick, 2000). The 11 day mission mapped approximately 80% of the global landmass using C-band ( $\lambda = 5.6$  cm) and X-band ( $\lambda = 3.0$  cm) wavelengths. SRTM specifications have an absolute vertical accuracy of 16 m, a relative vertical accuracy of 10 m, and an absolute horizontal accuracy of 20 m (Balmer, 1999). The C-band frequencies do not penetrate vegetation, so the canopy height is added to the ground elevation (Falorni *et al.*, 2005). Consequently, SRTM elevations generally reflect the height of the tallest feature on the ground, natural or built. Because the data were gathered in 2000, they are more current than NED. This, for example, is an advantage over urban areas and mining or quarrying areas. SRTM also has a resolution of 1 arcsec on a global scale. However, the average elevation error in the SRTM dataset is generally greater than that of NED, particularly at shorter scales (less than  $\sim 200$  m; Smith and Sandwell, 2003).

The key difference between the two datasets is that NED attempts to map the ground surface, whereas SRTM is canopy based (USGS, 2008). Because we are concerned with surficial effects from earthquakes and resolving the topographic gradient of the near-surface geology, it follows that a bare-earth elevation model will better suit our applications. However, we investigate the use of both datasets in this study. Both the NED and SRTM datasets are available for download from the National Map Seamless Server in Environmental Systems Research Institute (ESRI) ArcMap™ grid format.

In typical ShakeMap applications, we do not require  $V_{S30}$  to be defined at resolutions as great as 30 m grid spacing. Furthermore, the use of the highest resolution 1 arcsec data results in limitations in data handling and conversion for regional site-condition mapping because of the volume of data required. Consequently, we use the NED DEM at a resolution of 3 arcsec (approximately 90 m) for the San Francisco Bay area, Los Angeles (not shown here), and St. Louis. The DEMs are exported from ArcMap to a text file and are subsequently converted to a Generic Mapping Tools (Wessel and Smith, 1991) grid file for further analyses. We downsample each of the 3 arcsec (3c) grid files to a second grid with a resolution of 9 arcsec (9c) over the same spatial area.

### Modification of Slope- $V_{S30}$ Correlations

Initial testing in the San Francisco Bay area clearly indicated that the current slope- $V_{S30}$  correlations of Wald and Allen (2007) do not hold for higher-resolution topography data, particularly at steeper gradients. This is because the higher-resolution data allow for consistently higher gradients to be resolved because the lower sampling rates of the 30c dataset inherently smooth maximum slope values returned from topography. Consequently, consistently higher  $V_{S30}$  ve-

locities are predicted using the high-resolution data in the higher slope regions using the existing 30c slope- $V_{S30}$  correlations (Fig. 1).

Differences in the lower slope regions are less apparent because these landscapes can be equally well-sampled using the lower-resolution 30c dataset; thus, similar gradients are

recovered to the higher-resolution data. These are the regions where it is most important to obtain reliable estimates of  $V_{S30}$  because the low velocities estimated from low gradients will tend to amplify strong ground shaking more than regions of higher gradients. Statistical analysis of the observed and predicted values for all of California clearly demonstrates that

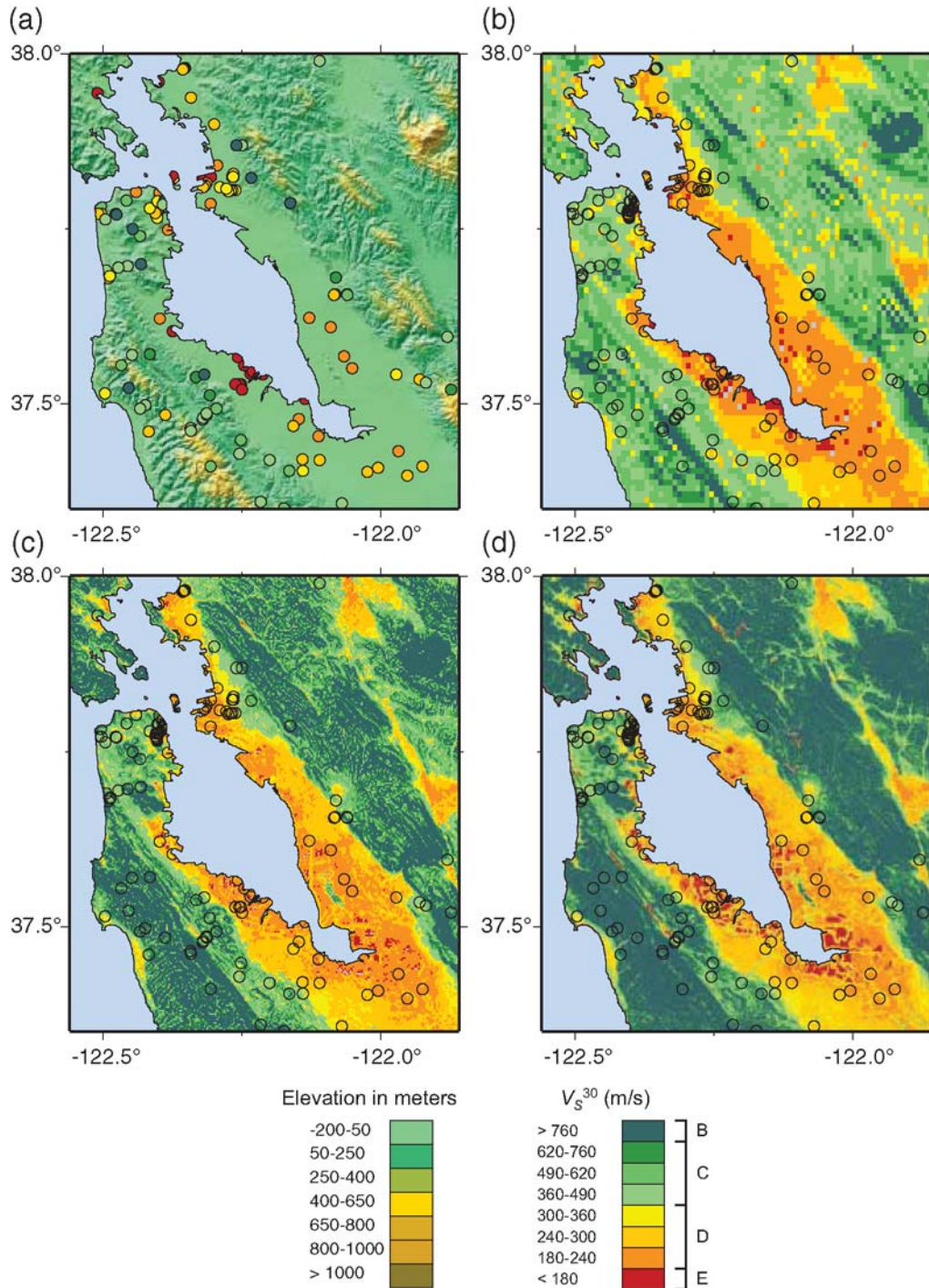


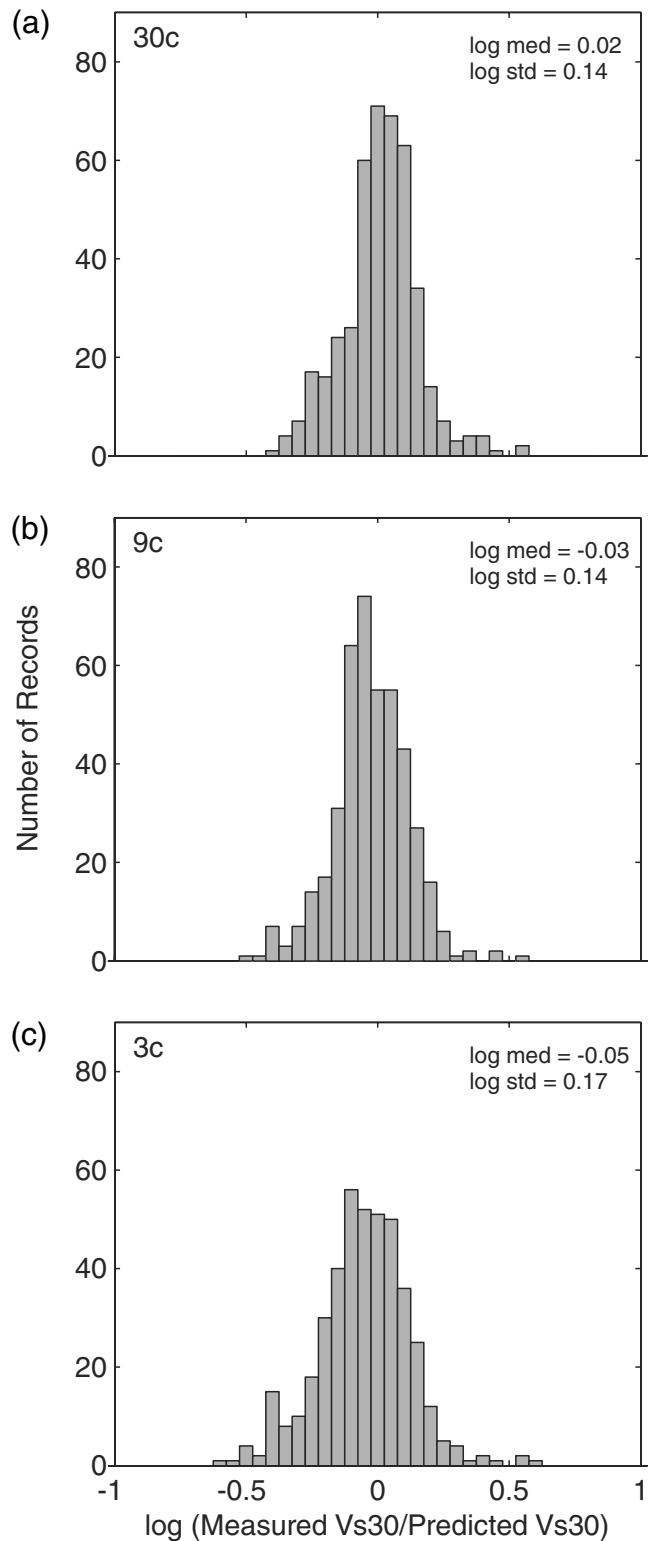
**Figure 1.** (a) Elevation of the San Francisco Bay area, superimposed with shear velocity measurements (circles) color-coded by  $V_{S30}$ . (b)  $V_{S30}$  map based on the modified SRTM 30c slope- $V_{S30}$  correlations of Wald and Allen (2007). (c)  $V_{S30}$  map based on NED 9c and (d) 3c. Both 9c and 3c maps use the 30c SRTM slope- $V_{S30}$  correlations. Note that the NED-based maps predict consistently higher velocities in the regions of high relief using the 30c correlations. Hollow circles in latter maps indicate the locations of  $V_{S30}$  measurements indicated in (a).

the higher-resolution datasets overestimate  $V_{S30}$  relative to the 30c SRTM data. Comparing the distribution of the residuals with the existing 30c correlations indicates that there is a similar variance in the predicted values from both the 9c NED and 30c SRTM maps (Fig. 2a,b). The 3c map results in a wider distribution in the comparison of observed and predicted  $V_{S30}$  (Fig. 2c).

The slope- $V_{S30}$  correlations were modified for the 9c data (Table 1) using the methods described in Wald and Allen (2007). The residual  $V_{S30}$  estimates for the 3c and 9c NED datasets using these new 9c correlations were subsequently recalculated (Fig. 3). Note that the median residual value for the 9c dataset is close to zero. However, the scatter in the residuals does not significantly improve and is similar to that calculated from the 30c SRTM data (Fig. 2a). The median residual for the 3c dataset moves closer to zero, indicating a slightly smaller misfit to the measured  $V_{S30}$  data. However, the variance of the residuals does not noticeably improve. From this result, we infer that the use of higher-resolution DEMs may have diminishing returns in resolving  $V_{S30}$  estimates because the higher data sampling introduces more variable gradients. Consequently, it may not be as good a predictor of  $V_{S30}$  as the smoothed lower-resolution DEMs. Conversely, one benefit of the higher-resolution data over the 30c STRM data is that smaller geological features can be resolved. For example, Coyote Hills in the southeast of the San Francisco Bay area can be clearly identified in the higher-resolution 9c DEM (Fig. 4), but is barely apparent in the 30c dataset (Fig. 1b).

In attempting to resolve differences between the 9c and 30c correlations, we note that the original 30c active tectonic correlations of Wald and Allen (2007) slightly overestimated  $V_{S30}$  for sites measured on low gradients. This, in combination with a slight underestimation of  $V_{S30}$  on higher slopes, resulted in an overall net residual of near zero in our original study. This effect was not identified until measured  $V_{S30}$  data in different velocity ranges were analyzed in more detail. The overall difference between these correlations is minor and should not significantly affect hazard calculations based on the original 30c correlations (Wald and Allen, 2007). The modified slope- $V_{S30}$  correlations for 30c SRTM data are also indicated in Table 1. Note that the 9c and modified 30c active tectonic correlations are now almost identical for National Earthquake Hazard Reduction Program (NEHRP) site classes *E* and *D* (Building Seismic Safety Council, 2004).

We now compare the amplification potential across the SRTM 30c and calibrated NED 9c maps. Amplification for midperiods of ground motion is assigned to each grid cell by applying the amplification factors of Borcherdt (1994), assuming a uniform peak ground acceleration of  $250 \text{ cm/sec}^2$ . Next, we take the ratio of the two maps to examine the relative difference in amplification (Fig. 5). We clearly observe that the 9c topography data yield higher velocities (and thus lower amplification) in the steeper regions of the map. The other key difference is higher amplification in the NED-based map at hill-basin transitions, such as along



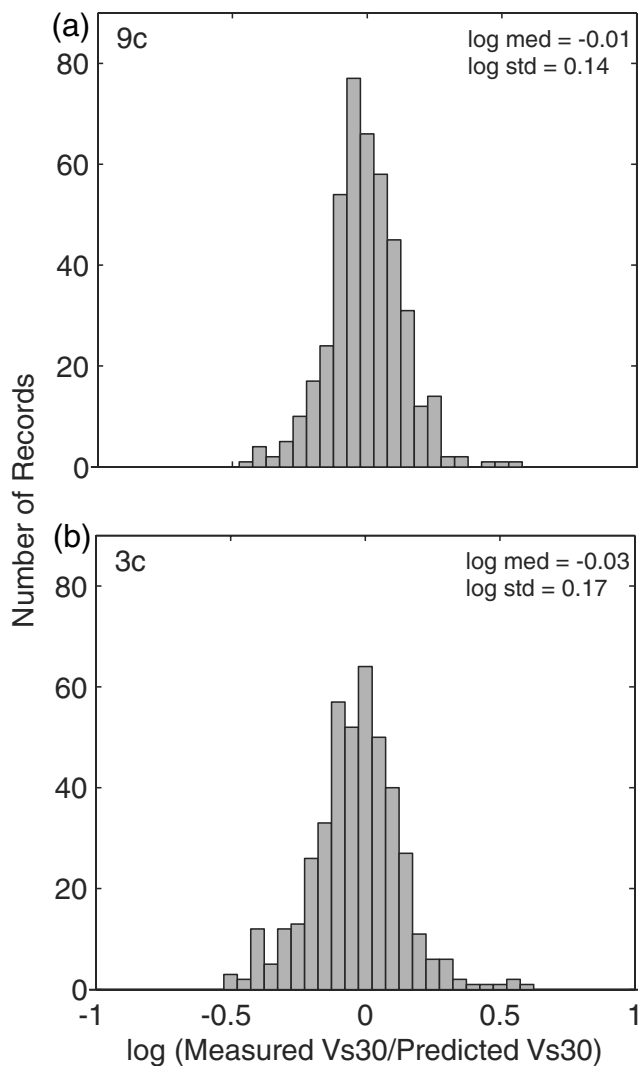
**Figure 2.** Histograms showing differences of measured Californian (both San Francisco Bay and Los Angeles regions)  $V_{S30}$  values compared with (a) values derived from SRTM 30c elevation data, (b) NED 9c data, and (c) NED 3c data. All comparisons use the modified 30c slope- $V_{S30}$  correlations. Note that the 30c correlations tend to overestimate  $V_{S30}$  for higher-resolution data. Median values near zero indicate a good correlation between observed and predicted values.

Table 1

Correlations between Topographic Gradient and  $V_{S30}$  Using the NED 9c Digital Elevation Models for the National Earthquake Hazard Reduction Program (NEHRP) Site Classes

NEHRP Site Class	$V_{S30}$ Range (m/sec)	9 arcsec Gradient Range (m/m) (Active Tectonic)	9 arcsec Gradient Range (m/m) (Stable Continent)	Modified 30 arcsec Gradient Range (m/m) (Active Tectonic)
E	< 180	$< 3 \times 10^{-4}$	$< 1 \times 10^{-4}$	$< 3 \times 10^{-4}$
	180–240	$3 \times 10^{-4}$ – $3.5 \times 10^{-3}$	$1 \times 10^{-4}$ – $8.5 \times 10^{-3}$	$3 \times 10^{-4}$ – $3.5 \times 10^{-3}$
D	240–300	$3.5 \times 10^{-3}$ –0.010	$4.5 \times 10^{-3}$ – $8.5 \times 10^{-3}$	$3.5 \times 10^{-3}$ –0.010
	300–360	0.010–0.024	$8.5 \times 10^{-3}$ –0.013	0.010–0.018
	360–490	0.024–0.08	0.013–0.022	0.018–0.05
C	490–620	0.08–0.14	0.022–0.03	0.05–0.10
	620–760	0.14–0.20	0.03–0.04	0.10–0.14
B	> 760	> 0.20	> 0.04	> 0.14

New correlations are developed for active tectonic and stable continental regions. Also indicated are the modified correlations to Wald and Allen’s (2007) original slope- $V_{S30}$  correlations for the 30c SRTM data.



**Figure 3.** Histograms showing differences of measured Californian  $V_{S30}$  values compared with (a) values derived from NED 9c data and (b) NED 3c data. Comparisons use the new 9c slope- $V_{S30}$  correlations. The median and scatter of the 9c data are now comparable with the 30c topographic data (Fig. 2a). The misfit for the 3c data decreases but still indicates a larger variance in the observed-to-predicted comparison.

the Hayward fault in the east bay region. This is because the higher-resolution topography is able to resolve changes in slope in greater detail; thus, it can better delineate these boundaries.

### Application in Stable Continental Settings

Based on the aforementioned observations for the San Francisco Bay area, we compare the 30c SRTM topography against the 9c NED for the stable continental setting of

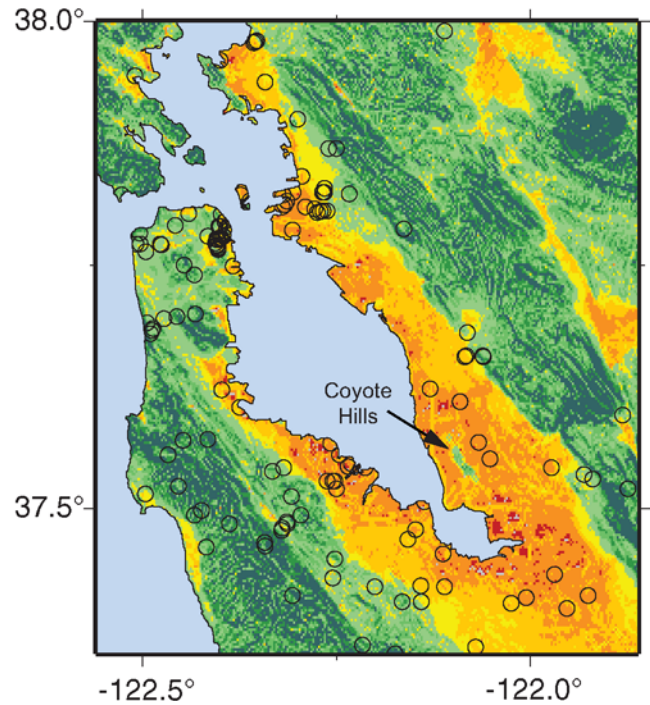


**Figure 4.** NED 9c  $V_{S30}$  map using the new 9c slope- $V_{S30}$  correlations. Note that the new correlations predict lower  $V_{S30}$  values in the hillier (high-velocity) regions than the map produced using the 30c correlations (Fig. 2c). Open circles represent localities of  $V_{S30}$  measurements (compare with Fig. 1a). As an example of the improved resolution, the Coyote Hills outcrop is clearly observed in this figure but is barely apparent in the SRTM 30c topography data (Fig. 1b). See Figure 1 for a map legend.

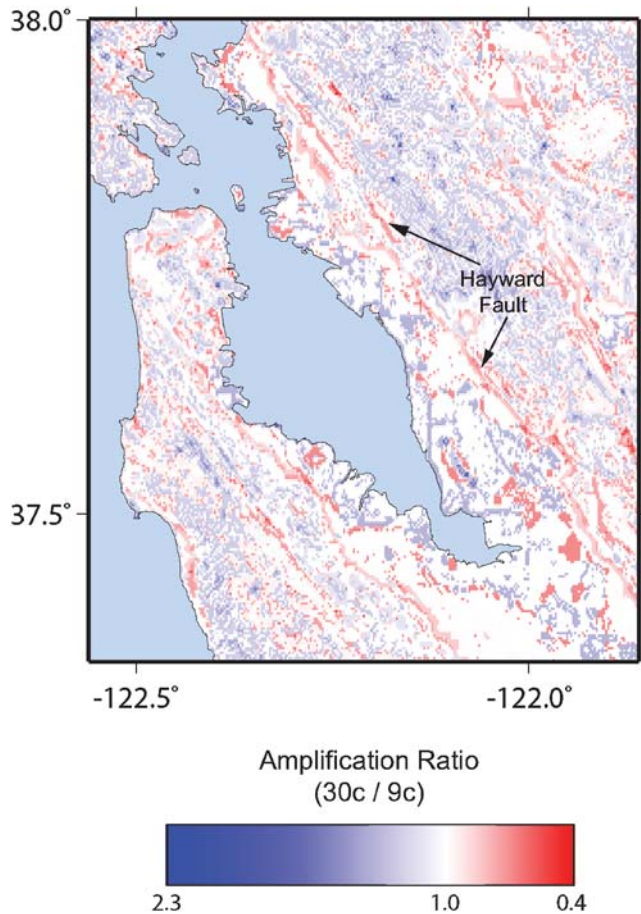


**Figure 5.** The ratio of the predicted amplification for a uniform PGA of  $250 \text{ cm/sec}^2$  assuming the Borchardt (1994) amplification factors for the 30c SRTM and 9c NED  $V_{S30}$  maps. Blue regions indicate where the 30c SRTM-based map predicts higher amplification, red regions indicate where higher amplifications are predicted from the 9c NED-based map, and white regions indicate where the two  $V_{S30}$  maps predict similar amplifications. Regions of similar amplification are most commonly areas of low gradient. Overall, the 9c  $V_{S30}$  map consistently predicts lower amplifications in the higher relief regions that bound the San Francisco Bay area. The 9c map also indicates improved delineation of hill–basin transitions, which are indicated by the northwest–southeast trending lineations of increased amplification potential. The example along the Hayward fault is indicated.

St. Louis, Missouri. Because Wald and Allen (2007) developed separate slope- $V_{S30}$  correlations for stable continental regions, it was necessary to also modify the original coefficients for the 9c DEM (Table 1). Using the NED-based map, drainage features in the region become more defined than on the SRTM-based map, as do the banks and terraces that bound the Mississippi River (Fig. 6).

Shallow shear velocity measurements in St. Louis recently gathered by Williams *et al.* (2007) were used to visually compare with our  $V_{S30}$  map. In general, the  $V_{S30}$  map and the measurements compare well with each other. Some differences are apparent on the east bank of the Mississippi River where softer aeolian sediments predominate (R. Williams, personal comm., 2008).

## Global Applications

We now focus on the use of the 9c SRTM data for higher-resolution global estimates of  $V_{S30}$ . The specific example we focus on is for the city of Taipei, Taiwan, for which there are abundant  $V_{S30}$  measurements (Chiou *et al.*, 2008). We apply the coefficients developed using the NED dataset in California to the 9c SRTM DEM for the Taipei region (Fig. 7). The most apparent observation from this dataset is that low slopes are poorly resolved. This is largely because the SRTM provides a canopy-based model of the Earth. These measurements are more variable than the bare-earth mapping methods of NED, particularly at low gradients. The same resolution SRTM dataset was tested for the San Francisco Bay area (not shown here) and indicated similar artifacts at low gradients. It is likely that these artifacts in the SRTM not only reflect vegetation, but also the canopy of the built environment. Consequently, we consider SRTM as a relatively poor predictor of  $V_{S30}$  at high resolutions. However, we still consider the down-sampled global SRTM 30c elevation dataset to be a reliable predictor of  $V_{S30}$  (Wald and Allen, 2007) because the small-scale variations in elevation that are abundant in the high-resolution data are smoothed. Consequently, the 30c maps are less sensitive to minor perturbations in gradient that are abundant in the higher-resolution SRTM data.

## Discussion

In general, we observe that the use of higher-resolution topographic data has potential for providing improved estimates of seismic site conditions ( $V_{S30}$ ) in regions with youthful and dynamic topographic landscapes where significant contrasts in topographic gradient exist (e.g., transitions between steep hill slopes and flat basins). There is also improved delineation of geologic and geomorphic features (e.g., drainage systems, rock outcrops, etc.), which may be representative of changes in  $V_{S30}$ . However, the use of higher-resolution data appears to provide little to no improvement in the median residuals of observed to predicted  $V_{S30}$ . Furthermore, there are diminishing returns in using resolutions finer than 9 arcsec because they tend to introduce more variability in slope calculations and thus reduce confidence in the correlation with the measured  $V_{S30}$  data (see Figs. 2c and 3b). In addition, the lower-resolution 30c data provide comparable estimates of  $V_{S30}$  to the 9c data.

The use of higher-resolution topography data can resolve smaller differences in gradient at higher slopes and is consequently better as a predictive tool in these areas. Conversely, it is less important to obtain accurate estimates of  $V_{S30}$  in these areas because high-relief (or faster  $V_{S30}$ ) regions are less likely to amplify ground shaking. In this study, we do not consider topographic effects, which have been observed to focus and amplify ground motions on steeper hill slopes in some instances (e.g., Dowrick, 1998). Differences between high and low resolution DEMs in the low-gradient regions, where resolving  $V_{S30}$  is likely to be more important,

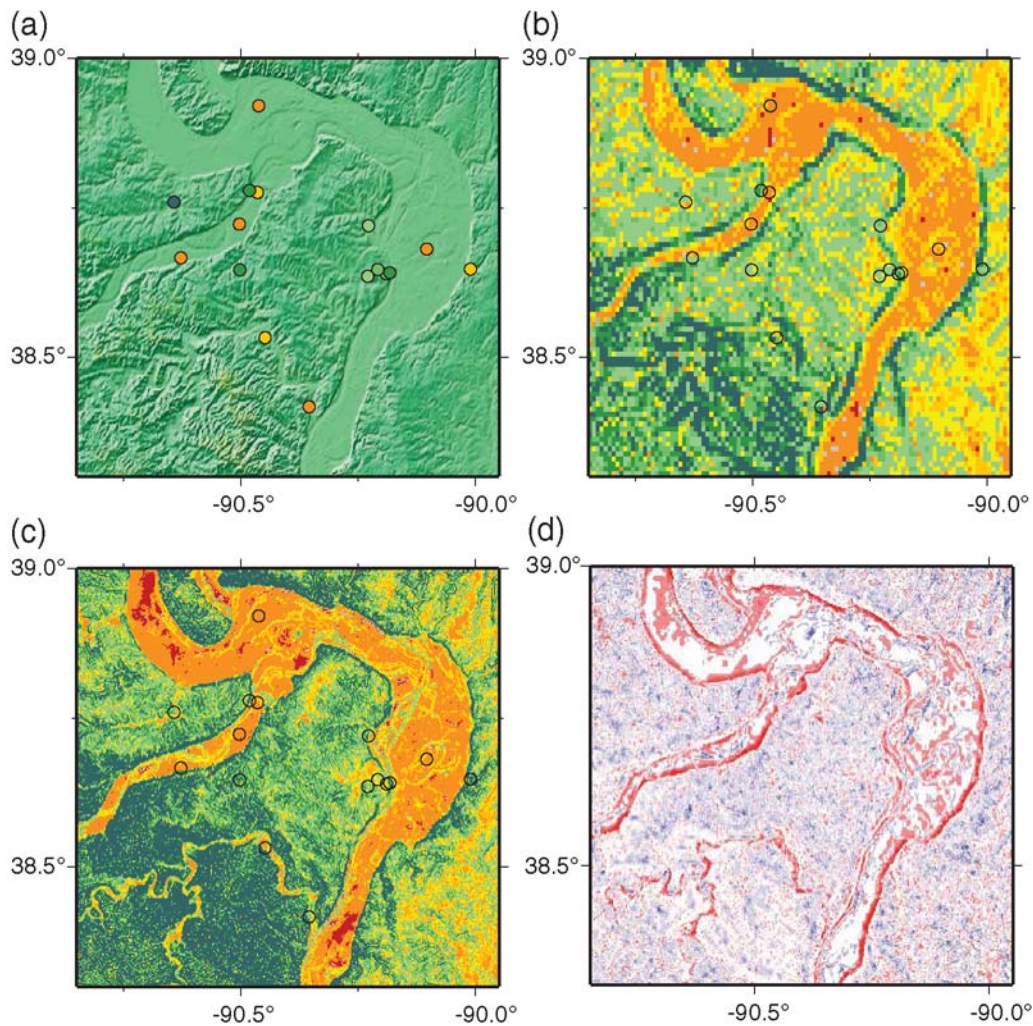


**Figure 6.** (a) Elevation of the St. Louis, Missouri, area superimposed with shear velocity measurements of Williams *et al.* (2007) color-coded by  $V_{S30}$ . (b)  $V_{S30}$  map based on the SRTM 30c stable continent slope- $V_{S30}$  correlations. (c)  $V_{S30}$  map based on NED 9c using the new 9c NED slope- $V_{S30}$  correlations for stable continental regions. Hollow circles in maps (b) and (c) indicate the locations of  $V_{S30}$  measurements indicated in (a). In the NED-based map, drainage features in the region become more defined than on the SRTM-based map, as do the steep bluffs that bound the Mississippi River flood plain. (d) The ratio of the predicted amplification for the 30c SRTM and 9c NED  $V_{S30}$  maps tends to highlight the boundaries of major drainage features and floodplains. See Figures 1 and 5 for map legends.

are not as obvious because the wavelength of the landscape is adequately sampled by each of the elevation models. Moreover, the inherent smoothing that occurs in the lower-resolution topographic data may actually provide more stable estimates of  $V_{S30}$ , removing minor perturbations in the gradient that may not necessarily represent real changes in the physical properties of the surficial geology.

The  $V_{S30}$  measurements against which we are calibrating are collected using numerous techniques for a variety of geotechnical purposes and thus may not be internally consistent. Consequently, these data may have significant uncertainties and should not be overinterpreted when correlating against high-resolution topographic data. Finally, the use of high-resolution topography data across large spatial extents may result in slower computation time for real-time earthquake alert systems owing to the volume of data being processed. For Global ShakeMap and PAGER applications,

obtaining timely estimates of earthquake shaking and its potential impact are important, and the use of these high-resolution data may delay the delivery of earthquake alerts.

$V_{S30}$  is not the only factor controlling ground-motion amplification. In addition to the previously noted topographic effects, the effects of deep sedimentary basins can also greatly modify the level of ground shaking observed at sites located within them and thus should be considered in combination with shallow seismic site conditions. At present, a method that can automatically delineate sedimentary basins from topographic data alone has not been developed. However, it should be possible to fit simple geometric shapes (e.g., ellipses) at the transition of hills and basins by using the average slope of the hills surrounding the basin as a crude predictor of three-dimensional basin geometry. It is likely that this approach will only be valid in regions where large contrasts in hill and basin slopes exist. We are also investi-

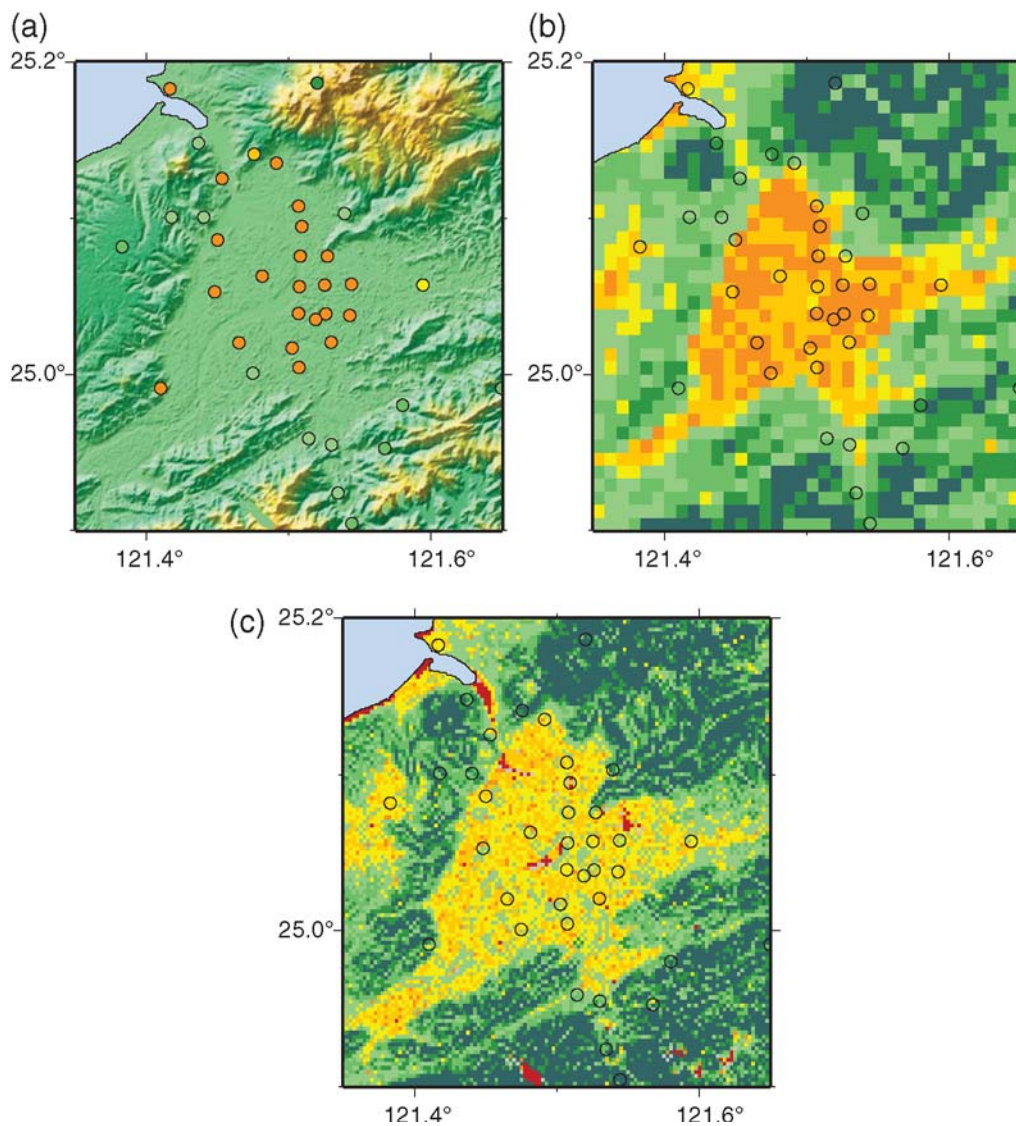


**Figure 7.** An example of using higher-resolution SRTM digital elevation models for resolving  $V_{S30}$  for the Taipei, Taiwan, region. (a) Elevation of the Taipei region, superimposed with shear velocity measurements color-coded by  $V_{S30}$ . (b)  $V_{S30}$  map based on the modified SRTM 30c slope- $V_{S30}$  using 30c SRTM data. (c)  $V_{S30}$  map from the 9c SRTM DEM using the 9c NED slope- $V_{S30}$  correlations for active tectonic regions. We observe that low gradients in the 9c SRTM are poorly resolved. This is largely because the SRTM provides canopy-based maps that have more artifacts and produce more variable gradients than the earth-based mapping methods of NED, particularly at low gradients. See Figure 1 for map legends.

gating the potential for using these topography data for rapid liquefaction-susceptibility mapping immediately following a global earthquake to supplement PAGER loss estimates. This could be a useful tool for disaster response planning and provide important information regarding the potential condition and recovery times of crucial lifelines such as road and rail networks or ports.

#### Data and Resources

DEMs used in this study were obtained from the USGS EROS Data Center's National Map Seamless Server, available at <http://seamless.usgs.gov/> (last accessed on 13 November 2008). Californian  $V_{S30}$  measurements were

obtained from Chris Wills (2006) via written communications. Taiwanese  $V_{S30}$  measurements were obtained from the Pacific Earthquake Engineering Research Center's Next Generation Attenuation strong-motion database (Chiou *et al.*, 2008), available for download at <http://peer.berkeley.edu/nga/> (last accessed on 13 November 2008). All maps were produced using Generic Mapping Tools (Wessel and Smith, 1991).

#### Acknowledgments

We are grateful to Jonathan Godt, Chris Wills, Andrew McPherson, Kuowan Lin, and Ned Field for their reviews that significantly improved the manuscript. We thank Rob Williams and Martin Messmer for discussions on the utility and accuracy of the St. Louis site-conditions map. Funding for

this research was provided, in part, by a grant from the U.S. Agency for International Development.

## References

- Allen, T. I., and D. J. Wald (2007). Topographic slope as a proxy for seismic site-conditions ( $V_{S30}$ ) and amplification around the globe, *U.S. Geol. Surv. Open-File Rept. 2007-1357*, 69 pp.
- Balmer, R. (1999). The SRTM mission—a worldwide 30 m resolution DEM from SAR interferometry in 11 days, in the *Proceedings of the 47th Photogrammetric Week '99*, D. Fritsch and R. Spiller (Editors), Wichmann Verlag, Heidelberg, 145–154.
- Borcherdt, R. D. (1994). Estimates of site-dependent response spectra for design (methodology and justification), *Earthq. Spectra* **10**, 617–653.
- Building Seismic Safety Council (2004). NEHRP recommended provisions for seismic regulations for new buildings and other structures, 2003 Ed., Federal Emergency Management Agency, Washington, D.C., Vol. **450**, 338 pp.
- Bungum, H., E. Harmandar, V. Oye, C. D. Lindholm, and B. Etzelmuller (2007). Adapting ShakeMap to Europe: ground-motion relations and soil response (Abstract S51A-0229), *Eos Trans. AGU* **88** (Fall Meet. Suppl.), S51A-0229.
- Chiou, B., R. Darragh, N. Gregor, and W. Silva (2008). NGA project strong-motion database, *Earthq. Spectra* **24**, 23–44.
- Dowrick, D. J. (1998). Damage and intensities in the magnitude 7.8 1931 Hawke's Bay, New Zealand earthquake, *Bull. N. Z. Nat. Soc. Earthq. Eng.* **31**, 139–163.
- Earle, P. S., D. J. Wald, T. I. Allen, K. S. Jaiswal, K. A. Porter, and M. G. Hearne (2008). Rapid exposure and loss estimates for the May 12, 2008  $M_W$  7.9 Wenchuan earthquake provided by the U.S. Geological Survey's PAGER system, in the *14th World Conference on Earthquake Engineering*, Beijing, China, Paper S31-039.
- Falorni, G., V. Teles, E. R. Vivoni, R. L. Bras, and K. S. Amaratunga (2005). Analysis and characterization of the vertical accuracy of digital elevation models from the Shuttle Radar Topography Mission, *J. Geophys. Res.* **110**, F02005, doi 10.1029/2003JF000113.
- Farr, T. G., and M. Kobrick (2000). Shuttle Radar Topography Mission produces a wealth of data, *Eos Trans. AGU* **81**, 583–585.
- Gallant, J. C., and T. I. Dowling (2003). A multiresolution index of valley bottom flatness for mapping depositional areas, *Water Resour. Res.* **39**, no. 12, 1347, doi 10.1029/2002WR001426.
- Gesch, D., M. Oimoen, S. Greenlee, C. Nelson, M. Steuck, and D. Tyler (2002). The National Elevation Dataset, *Photogramm. Eng. Rem. Sens.* **68**, no. 1, available at <http://www.asprs.org/publications/pers/2002journal/january/highlight.html> (last accessed December 2008).
- Harmandar, E., V. Oye, C. Lindholm, and H. Bungum (2007). Soil condition maps based on topographic slope, Network of Earthquake Research Institutes for Earthquake Seismology (NERIES) JRA3 Report, 20 pp.
- Ionescu, C., A. Danet, M. B. Sorensen, B. Zaharia, D. Stromeyer, and G. Grunthal (2007). Implementation of the near real time ShakeMap system in Romania (Abstract S51A-0215), *Eos Trans. AGU* **88** (Fall Meet. Suppl.), S51A-0215.
- Michelini, A., L. Faenza, V. Lauciani, and L. Malagnini (2008). ShakeMap implementation in Italy, *Seism. Res. Lett.* **79**, 688–697.
- Smith, B., and D. Sandwell (2003). Accuracy and resolution of shuttle radar topography mission data, *Geophys. Res. Lett.* **30**, 1467, doi 10.1029/2002GL016643.
- U.S. Geological Survey (2008). *The National Map Seamless Server*, available at <http://seamless.usgs.gov/index.php> (last accessed June 2008).
- Wald, D. J., and T. I. Allen (2007). Topographic slope as a proxy for seismic site conditions and amplification, *Bull. Seismol. Soc. Am.* **97**, 1379–1395.
- Wald, D. J., P. S. Earle, T. I. Allen, K. Jaiswal, K. Porter, and M. Hearne (2008). Development of the U.S. Geological Survey's PAGER system (Prompt Assessment of Global Earthquakes for Response), in the *14th World Conference on Earthquake Engineering*, Beijing, China, Paper 10-0008.
- Wald, D. J., V. Quitoriano, T. H. Heaton, H. Kanamori, C. W. Scrivner, and B. C. Worden (1999). TriNet "ShakeMaps": rapid generation of peak ground-motion and intensity maps for earthquakes in southern California, *Earthq. Spectra* **15**, 537–556.
- Wessel, P., and W. H. F. Smith (1991). Generic Mapping Tools, *Eos Trans. AGU* **72**, 441.
- Williams, R. A., J. K. Odum, W. J. Stephenson, and R. B. Herrmann (2007). Shallow  $P$ - and  $S$ -wave velocities and site resonances in the St. Louis region, Missouri-Illinois, *Earthq. Spectra* **23**, 711–726.
- Wills, C., and C. Gutierrez (2008). Investigation of geographic rules for improving site-conditions mapping, *Calif. Geol. Surv. Final Tech. Rept.*, 20 pp. (Award No. 07HQGR0061).

National Earthquake Information Center  
U.S. Geological Survey  
1711 Illinois Avenue  
Golden, Colorado 80401

Manuscript received 27 August 2008